

REACTIVITY OF COAL AND CHAR IN CO₂ ATMOSPHERE

S. Dutta, C. Y. Wen and R. J. Belt*

Department of Chemical Engineering, West Virginia University, Morgantown, WV 26506

*ERDA, Morgantown Energy Research Center, Collins Ferry Road, Morgantown, WV 26506

Abstract - Reactivities of a few raw coals and chars of these coals obtained from gasifiers operating under different conditions have been measured in CO₂ at the temperatures 1550-2000°F. The reactivities have been measured in a thermogravimetric analyzer up to complete conversions of the samples in most cases. Properties like surface area, pore size distribution, porosity and density have been determined for each sample. Actual pore structures of a few samples have been observed at different conversion levels by a scanning electron microscope. In order to compare the reactivities of different samples, the char-gasification process has been divided into two distinct stages: the first stage due to pyrolysis and the second stage due to char-CO₂ reaction. Reactivities due to the first stage can be roughly related to volatile matter contents of the solids and the rate of heating. Through an Arrhenius type equation, an activation energy of about 2.5 Kcal/mole is obtained for the first stage. The reactivity of a char in the second stage is found to depend more on its coal seam than on the gasification scheme used in its production. Activation energy for the second stage reaction has been found to be about 59 Kcal/mole. A rate equation has been proposed for the second stage that incorporates the effect of relative available pore surface area changing during reaction. The rate conversion curves calculated from this equation fit well with the experimental data.

Introduction

A proper understanding of the coal/char gasification kinetics is essential for successful design of a gasifier. Effects of temperature, pressure and gaseous environments on the rate of gasification of coal/char have been extensively studied by various investigators. In addition, the rate depends also on the nature and origin of the coal or char itself. The pore characteristics and hence the reactivity of a char have been found to vary not only with the maceral of its parent coal but also with the history of its genesis, i.e., the temperature, pressure, rate of heating and gaseous environments, etc., prevailed during its formation. The present study is devoted to determination of reactivities of a few coal and char samples which are produced in some pilot plant experiments conducted under different gasification schemes. This investigation will help find the relationship, if any, between the reactivities and the physical characteristics of the samples.

In the present investigation reactivities are measured in a flowing stream of pure CO₂ at the atmospheric pressure. The rate of C-CO₂ reaction has been studied by various investigators^(1,5,7,9,10,12,13). However, considerable discrepancy has been reported between the values of activation energy of this reaction, ranging from 48 to 86 Kcal/mole.

Pyrolysis of coal or char takes place prior to or concurrent with other reactions in a gasifier. The behavior of pyrolysis is not yet properly established. It is, however, known that the rate of pyrolysis and the amount and composition of volatile products from a given sample of coal or char depends on several factors⁽³⁾ such as (a) rate of heating, (b) final decomposition temperature attained, (c) vapor residence time and (d) the environment under which the pyrolysis takes place. In the present investigation pyrolysis of coal and char in a CO₂ atmosphere can be studied separately from CO₂ reaction. This is due to the fact that pyrolysis normally starts at about 350-400°C and is almost complete at about 1000°C⁽²⁾ within seconds, whereas the C-CO₂ reaction is hardly detectable below 800-900°C. Therefore, at a moderate rate of heating, the two stages, the pyrolysis and the char-CO₂ reaction, will be separable from each other, the latter starting only after the former stage is essentially

complete. The char-CO₂ reaction after the pyrolysis reaction is completed takes place on char surface and is essentially carbon-CO₂ reaction.

Gulbransen and Andrew⁽⁴⁾ showed that the internal surface area of graphite increases markedly during reaction with both oxygen and CO₂. Walker, Foresti and Wright⁽¹⁰⁾ made the detailed study on the possible correlation existing between reaction rates and changes in surface area during reaction. They concluded that the reaction develops new surface by enlarging to some extent the micropores of the solid but principally by opening up pore volume not previously available to reactant gas because the microcapillaries were too small or because existing pores were unconnected. During the reaction surface area increases up to a point when the rate of formation of new area is paralleled by the rate of destruction of old area. Surface area decreases on further conversion. For graphite-CO₂ reaction, Petersen, Walker and Wright⁽⁶⁾ found that the observed rates were not simple functions of the total available surface area, as determined by the low temperature gas adsorption technique, as might be expected if the reaction was chemical reaction controlled.

Turkdogan, et.al.⁽⁸⁾ made a detailed investigation on the pore characteristics of several forms of carbon. Their studies indicate that depending on the type of carbon, about 1/4 to 1/2 of the volume is isolated by micropores and hence is not available for reaction at the beginning. The surface areas of carbon investigated by them covered a large range from 0.1 to 1100 m²/g. In all cases, most of the internal area was attributed to the micropores, 10-50 Å dia.

Experimental

A Fisher TGA apparatus (model 120P) was used in the present investigation. Two coal samples (one from Pittsburgh seam and the other from Illinois seam) and four char samples derived from these coals under different gasification schemes were investigated.

To start a run 15-30 mg. of coal or char particles of -35+60 mesh were placed in the platinum holder hanging from one arm of the balance of the TGA. After fixing the hangdown tube in position, the system was first evacuated to about 20 mm Hg and then flushed with CO₂ at a flow rate of about 200 ml./min. for about two and a half hours. The outlet gas was analyzed by gas chromatograph to assure that it is air-free. The oven was preheated to the desired temperature. The CO₂ gas stream was turned to the desired flow rate (150 ml./min.) and the furnace was quickly raised to a prefixed level, to enclose the hang-down tube. The weight and the time derivative of weight loss of the sample and the sample temperature were recorded continuously throughout the experiment.

The porosity, density, pore volume and pore size distribution of the devolatilized chars and coals have been determined by mercury porosimetry using pressures up to 50,000 psi. The pore surface areas and pore size distribution of the samples have been determined by BET nitrogen adsorption method using NUMEC surface-area-apparatus, model AfA4. Moreover, the actual macropore matrix of a few of these samples have been visually observed, at several stages of their conversions, by a scanning electron microscope up to a magnification of 6,000.

Experimental Results and Discussions

Figure 1 is the reproduction of two typical chart recordings of the weight loss and the rate of weight loss curves by the TGA apparatus. In this figure the initial peaks in the rate curves are due to the very fast pyrolysis stage. After this stage, the second stage reaction begins which is comparatively slow and is mostly C-CO₂ reaction. The analyses of the chars just after the pyrolysis stage show carbon contents of 95-98% on an ash-free basis for all the six samples.

Figure 1 also shows an intermediate region, between the two vertical lines a and b, where not only the pyrolysis but also the second stage char-CO₂ reaction is affected by the heating rate of the sample. The sample temperature versus time for these two cases are shown in Figure 2. In these experiments the sample temperature is assumed to be identical with that recorded by an open thermocouple placed about 3 mm. from the surface of the reacting solid sample. The rate of gasification at the first and intermediate stages will obviously depend on the sample heating rate. Once the sample attains equilibrium temperature (approximately within 4 min. in the present case), the rest of the process proceeds essentially under isothermal condition.

A. The First Stage - Pyrolysis

The rate of gasification and the fraction conversion due to pyrolysis are shown for four samples in Figure 2. The total conversions obtained at this stage have been found to be nearly equal to the volatile matter contents of the chars and coals as determined by the proximate analyses. The conversion (f) in the first stage (pyrolysis) is defined here as that conversion which is attained at the almost-constant weight period (the region between the vertical lines a and b in Figure 2, immediately after the rapid weight loss at the start of the process. Such a constant-weight-period has been observed in almost all cases. Figure 2 also shows that the pyrolysis is almost complete before a temperature of about 1500°F is reached, while the char-CO₂ reaction is insignificant up to this temperature, as will be seen later.

The total conversion (f) from the pyrolysis stage increases with the increase in temperature. However, this increase (~1%) is not appreciable, at a particular heating rate, in the studied temperature range 1550-1975°F.

Figure 3 shows the effect of sample heating rate on the rate of pyrolysis of hydrane char #150. It is noted that the peak heights of these rate curves are roughly proportional to the average slopes of the heating rate curves.

A Pyrolysis Model: Pyrolysis cannot be considered as a single-step process involving a simple reaction. It occurs in stages or as "waves" of reactions involving many complex steps, which in turn vary from sample to sample and with the conditions of pyrolysis. No simple model would, therefore, represent this process completely. However, on an overall basis Wen et.al.⁽¹¹⁾ proposed an Arrhenius type equation as follows:

$$\frac{dx}{dt} = A e^{-B/RT} (f-x) \quad 1)$$

Following this equation, a plot of $(dx/dt)/(f-x)$ versus $1/T$ has been made with the values of dx/dt , f , x and T obtained from Figure 2. f is assumed constant in the studied temperature range. The plot is shown in Figure 4 for three char samples. The figure shows that no single straight line can be drawn through the points with certainty. This is partly due to the fact that the process is so fast that values of x , dx/dt at any instant cannot be read precisely from such rate and conversion curves shown in Figure 2.

Equation 1 has, therefore, been tested indirectly by assigning arbitrary values of A and B (in the ranges predicted by the points in Figure 4) and seeing whether the resulting values of x and dx/dt can match with the experimental ones. Since temperature is changing with time in this region, the values of x have been determined as a function of time from the following equation:

$$x = f \left[1 - e^{-A \int_0^t e^{-B/RT} dt} \right] \quad 2)$$

The evaluation of the integral in the above equation has been done numerically from known values of temperature (T) as a function of time (t). The rate, dx/dt , is next calculated from Equation 1. With $A=2,500$ cal/mole and $B=20.0$ min⁻¹, the predicted

conversion and rate curves for three chars have been found to match the experimental curves quite closely, as is shown in Figure 5a. The predicted curves and the experimental values for different heating rates are shown in Figure 5b. Calculations have been done only up to 1.5 min. in order to avoid the possible influence of the second stage process in the subsequent period.

The straight line drawn through the experimental points in Figure 4 are based on the above values of A and B.

Thus if the Arrhenius-type Equation 1 is assumed to approximate the pyrolysis stage, the value of activation energy becomes 2.5 Kcal/mole.

B. The Second Stage - Char-CO₂ Reaction

As has been mentioned earlier, the rate of pyrolysis or the first stage of char/coal gasification is very rapid and can be assumed nearly complete, when an almost-constant-weight period is attained in the weight-loss versus time curve. The remaining fraction of the solid reacts slowly with CO₂ which is termed the second stage of gasification. Although a small part of volatile matters may still remains with this fraction, this fraction consists essentially of carbon (95-98%), and ash. The rate, dx/dt , and conversion, x , are based on the reactive portion of char, which is the weight of solid remaining after the first stage less the weight of ash, and is termed as the base carbon.

Before studying the effect of temperature the effects of sample size, sample holder, particle size and gas (CO₂) flow rate on char gasification rate were examined.

Three kinds of sample holders of different sizes and shapes were tested using different amounts of samples placed on them. They were (a) a shallow petri-dish type holder of diameter 8.5 mm. and depth 2 mm., holding 3.75 mg. of sample, (b) a cup-shaped holder of mouth diameter 8.5 mm. and depth 7 mm., holding 18.5 mg. of sample and (c) a perforated cylindrical holder of diameter 6 mm. and depth 15 mm., holding 35.02 mg. of sample. No significant difference was found between the observed rates in the three cases at a gasification temperature of 1877°F and a gas flow rate of 150 ml/min. The cup-shaped sample holder was used in the rest of the experiments. Gas flow rates were varied in the range 42-210 ml/min., through the reactor tube of diameter 19 mm. No change in rate was observed at flow rates above 70 ml/min., at the gasification temperature of 1877°F. A flow-rate of 150 ml/min. was chosen for subsequent experiments. Particle size selected was -35+60 mesh, which showed negligible intraparticle diffusion resistance up to a temperature of about 1800°F.

Figures 6-11 show the rate versus conversion curves as a function of temperature for the six different samples studied. These figures also show the base carbon content of the chars at the fraction conversions indicated.

The experiments were conducted up to the complete conversions of the samples, except at lower temperatures where rates were extremely slow.

The Figures 6-11 clearly show that every sample has its own characteristic rate-conversion curve. For Hydrane Char #49, the curves can be considered linear (and passing through the origin) without significant error. However, for the other samples this is not true. Again for Hydrane Char #150, the rates are almost steady up to certain conversion levels, after which they decline. For Pittsburgh coal, rate-conversion curves show maxima at lower temperatures.

It is also noted that for the Pittsburgh coal and for the Hydrane Char #150, the nature of the curves changes also with temperature. This change is shown more clearly in Figure 12, where the rates are normalized with respect to the rates observed at 20% conversion level and plotted against conversion. The rate-conversion curve shows a maximum at lower temperatures only.

The variety of rate-conversion curves is due to the fact that different coal/char samples vary greatly from one another with respect to their pore structures and the change of such pore structures with conversion and temperature. To account for such phenomena, a term "a" is introduced into the rate equation, which represents the relative available pore surface area and is defined as follows:

$$a = \frac{\text{Available pore surface area per unit volume at any stage of conversion}}{\text{Initial available pore surface area per unit volume}}$$

The value of "a" varies with conversion and temperature. Ignoring the effect of temperature, the change of "a" with conversion, x, can be fitted into a function, up to x approaching unity, as follows:

$$a = 1 \pm 100 x^{\nu\beta} e^{-\beta x} \quad 0 \leq \nu \leq 1 \quad 3)$$

In this Equation ν and β are the physical parameters characteristic of a given coal or char. The value of ν indicates the conversion x at which the relative available surface area reaches the maximum or minimum value. According to this equation the relative available pore surface area of the particles may increase, decrease or may show a maximum or minimum as the reaction proceeds, according to the sign (+ or -) used in Equation 3. Since a drastic change in surface area and pore size would take place at the very end approaching complete conversion, the above Equation should not be applied beyond $x > 0.9$.

Therefore, the rate of disappearance of char due to CO_2 reaction, for chemical reaction control, may be expressed as

$$\frac{dx}{dt} = a k_v C_A (1-x) \quad 4)$$

Arrhenius-type temperature dependence is assumed for the rate constant, k_v , according to the following equation:

$$k_v = k_{v_0} e^{-E/RT} \quad 5)$$

In Figure 13, $(dx/dt)/C_A(1-x)$ at $x = 0.2$ are plotted against $1/T$. The values of ak_{v_0} and the activation energy E are determined from this plot. This Figure shows that the rates (at 20% conversion level) of Illinois seam Coal #6 and the three chars obtained from Illinois seam coal are significantly higher than those of Pittsburgh seam coal and the Hydrane Char #150 obtained from the Pittsburgh seam.

Among the four Illinois coal and chars, Synthane Char #122 appears to be the most reactive, although the difference in reactivity is not large.

The activation energy, E, is found to be 59.26 Kcal/mole for all coals and chars.

Equation 4 is applicable only when the chemical reaction rate controls the process. At higher temperature, however, diffusion resistance within the solid particles may become appreciable and therefore, an effectiveness factor must be introduced for such cases. Effectiveness factor, η , is defined here as follows:

$$\eta = \frac{\left(D_e \cdot \frac{dC_A}{dr} \right)_s 4\pi r_0^2}{(4/3\pi r_0^3) \{ a k_v \cdot C_{As} \cdot (1-x) \}} \quad 6)$$

If the change in effective diffusivity, D_e , during reaction is assumed negligible, Equation 6 can be solved by appropriate boundary conditions as follows:

$$\eta = \frac{3}{M} \left(\frac{1}{\tanh M} - \frac{1}{M} \right) \quad 7)$$

where $M = \phi_{vo} [(1-x)a]^{1/2}$

$$\text{and } \phi_{vo} = r_o \sqrt{\frac{k_v C_{So}}{D_e}}$$

For chemical reaction control, $\phi_{vo} = 0$. Thus, the rate of gasification with the influence of intraparticle diffusion is expressed as

$$\frac{dx}{dt} = \eta a k_v C_A (1-x) \quad 8)$$

Using the rate expression shown by Equation 8, the conversions are calculated for all the chars and coals tested. The calculated rates are compared with those observed from experimentation in Figures 6-11. The values of k_v , v , β and ϕ_{vo} used in these calculations are given in Table I. The calculated rates agree closely with experimental rates except that for Pittsburgh coal at higher temperatures. This may partly be due to the following reason. In contrast to the other coals and chars, the Pittsburgh coal is a highly caking coal having a swelling index of 8.5. These particles (-35+60 mesh) swell up to a considerable volume and agglomerate into a single lump during the pyrolysis stage. The whole sample (~20 mg) is thus glued together and reacts as a single particle of a considerably larger diameter. The change of porosity and hence the effective diffusivity in such a particle, as a function of conversion, may be appreciable deviating from assumptions made in the development of Equation 8.

As is indicated by Table I, the available surface area change with conversion is independent of temperature, in the studied range, for the Illinois seam coal and chars. However, for the Pittsburgh seam coal and char this change is a function of temperature. For the Pittsburgh seam coal and char the increase of available surface area appears to be less at higher temperature, for a particular conversion level.

Figure 14 shows how the relative available pore surface area "a" of the particles changes with conversion for different samples, in the temperature range 1600-1800°F.

Pore Characteristics of the Coal and Char Samples

The pore structures of Synthane Char #122, Hydrane Char #49, Hydrane Char #150 and Pittsburgh HVab coal have been observed through a scanning electron microscope, at several stages of their conversions in the range $x = 0 - 1$. The photographs taken at several magnifications (up to a maximum of 6,000) show that, as the reaction proceeds, the pores initially of a few microns (2-10 μ) in diameter, grow in size and bigger cavities are formed by the collapse of the solid linkage between the adjoining pore. The dimension of the solid particles have been observed to remain practically unchanged (except for the high swelling Pittsburgh seam coal) up to a conversion of about 80%. The highly porous matrix of the solid disintegrates into smaller fractions as the reaction proceeds further.

Table II shows the net pore volumes, volume-average pore diameters, densities and the porosities of the devolatilized samples as determined by the mercury penetration method on a Micromeritics' Model 905 0 - 50,000 psia Porosimeter. The average

TABLE I PHYSICAL AND RATE PARAMETERS USED IN CALCULATION FOR THE COAL AND CHAR SAMPLES

| Sample | $k_{v_0} \times 10^{-15}$, $\text{cm}^3/\text{mole-min.}$ | Temperature | v | β | ϕ_{v_0} |
|-----------------------------------------------------|------------------------------------------------------------|-------------|------|---------|--------------|
| IGT Char #HT155 (from Illinois Coal #6) | 0.113 | 1657-1922°F | 0.75 | 5.5 | 0 |
| Hydrane Char #49 (from Illinois Coal #6) | 0.123 | 1578-1938°F | 0.75 | 10.0 | 0 |
| Synthane Char #122 (from Illinois Coal #6) | 0.136 | 1565-1972°F | 0.75 | 6.0 | 0 |
| Illinois Coal #6 | 0.120 | 1569-1938°F | 0.75 | 6.0 | 0 |
| Hydrane Char #150 (from Pittsburgh HVab Coal) | 0.0670 | 1623°F | 1.0 | 4.4 | 0 |
| | | 1688°F | 1.0 | 4.4 | 0 |
| | | 1794°F | 1.0 | 4.7 | 0 |
| | | 1875°F | 1.0 | 5.0 | 2.5 |
| | | 1965°F | 1.0 | 5.5 | 4.2 |
| Pittsburgh HVab Coal | 0.0536 | 1682°F | 0.6 | 5.0 | 0 |
| | | 1742°F | 0.6 | 5.0 | 0 |
| | | 1778°F | 0.6 | 5.5 | 0 |
| | | 1888°F | 0.6 | 10.0 | 3.0 |
| | | 1952°F | 0.6 | 10.0 | 4.2 |

TABLE II. PORE CHARACTERISTICS OF COALS AND CHARs

| Devolatilized Samples | Properties Measured By Mercury Porosimetry | | | | Properties Measured by BET Method | |
|--------------------------|-----------------------------------------------|----------------------------------------------------|--------------------|----------|----------------------------------------------|-----------------------------------------------------------------------------------|
| | Net Pore Volume (cc/g) | Volume Average Pore Diameter (μ) | Density (g/cc.) | Porosity | Surface Area (m^2/g) | Surface Average Micropore Diameter, \bar{d}_{ps} , (\AA) |
| IGT Char #155 | 0.9200 | 9.2 | 1.54 | 0.767 | 423.87 | 11.61 |
| Hydrane Char #49 | 1.0344 | 2.3 | 1.43 | 0.765 | 171.69 | 22.34 |
| Synthane Char #122 | 2.1978 | 8.8 | 1.31 | 0.864 | 280.94 | 18.34 |
| Illinois Coal #6 | 2.6522 | 9.2 | 1.71 | 0.809 | 26.05 | -- |
| Hydrane Char #150 | 0.6463 | 2.4 | 1.53 | 0.655 | 18.04 | 106.00 |
| Pittsburgh HVab Coal | -- | -- | 2.11 | -- | 29.97 | -- |

pore diameters determined by this method agrees well with those observed by the scanning electron microscope.

Table II also shows the pore surface areas and the surface-average micro-pore diameters of devolatilized coal and char samples as determined by the BET nitrogen adsorption method. The surface-average micropore diameters (\bar{d}_{ps}) have been calculated from the measured micropore size distribution, according to the equation.

$$\bar{d}_{ps} = \frac{\sum d_{ps} \Delta A_p}{A_p}$$

where ΔA_p is the surface area occupied by the micropores of diameter d_{ps} and A_p is the total surface area of the solid.

These measurements show that although the bulk of void volumes of these coals and chars are occupied by comparatively large pores, several microns in diameter, almost all the surface areas determined by BET method are occupied by micropores, below 100-200 Å in diameter.

Reactivity of coal/char can be characterized by its intrinsic rate constant for the second stage reaction, k_{v_0} . The values of k_{v_0} (listed in Table I) apparently show no direct relationship with the measured pore surface areas. The pore surface areas and pore size distribution curves, however, show that higher surface areas are caused by the larger number of smaller pores. Calculations show that for the coal and char samples studied, only the fraction of surface area which is occupied by pores having diameter more than about 27.5 Å is available for reaction with CO_2 . The table below shows the surface areas covered by pores bigger than 27.5 Å, the total surface areas and the values of k_{v_0} for four chars.

| Sample | Surface Area (m^2/g) Covered by Pores Bigger Than 27.5 Å in dia. | Total Surface area (m^2/g) | $k_{v_0} \times 10^{-15}$ $cm^3/mole.min.$ |
|--------------------|----------------------------------------------------------------------------|--------------------------------------|-----------------------------------------------|
| Hydrane Char #150 | 18.75 | 18.75 | 0.0670 |
| IGT Char #HT155 | 25.43 | 423.87 | 0.113 |
| Hydrane Char #49 | 34.42 | 171.69 | 0.123 |
| Synthane Char #122 | 38.06 | 280.87 | 0.136 |

The reactivities are found to be almost proportional to the surface areas occupied by pores above 27.5 Å in diameter.

Conclusions

Gasification of coal/char in CO_2 atmosphere can be divided into two stages, the first stage due to pyrolysis and the second stage due to char- CO_2 reaction. Reactivity in the first stage is mainly a function of the volatile matter content of the char/coal and the rate of heating. The rate of pyrolysis can be approximated by an Arrhenius type expression (Equation 1) with an activation energy of about 2.5 Kcal/mole.

Reactivity of a char in the second stage char- CO_2 reaction, is found to depend more on its coal seam than on the gasification scheme used for its production. Each char/coal sample is found to have its own characteristic rate curve. The different rate characteristics of coals and chars are apparently due to the difference in their pore characteristics, which again change with conversion and temperature.

A parameter, that represents the change in available pore surface areas of the particles during reaction, is introduced into the rate equation to account for the rate-conversion curves. The calculated rates are found to agree quite well with the observed rates.

The rate of char-CO₂ reaction is found to have no direct relation with the total surface area of the pores. The study indicates that only a fraction of the total surface area which is occupied by pores above a certain diameter is available for reactions.

Notation

| | |
|----------------------------------|--------------------------------------------------------------------------------------------------|
| A | Pyrolysis rate constant, 1/min |
| A _p | Pore surface area, m ² /g |
| B ⁺ | Activation energy of pyrolysis, cal/cmole |
| C _A | Concentration of gas; C _{As} that at the outside surface of solid, mole/cm ³ |
| C _{So} | Initial solid concentration, mole/cm ³ |
| D _e | Effective diffusivity, cm ² /min |
| d _{ps} | Micropore diameter; d _{ps} surface average micropore diameter, Å |
| F | Total fraction conversion due to pyrolysis |
| k _v , k _{vo} | Second stage reaction rate constants, cm ³ /mole.min |
| R | Gas constant, cal/mole.°R |
| r | Radius of solid particle; r ₀ initial radius, cm |
| T | Temperature, °R |
| t | Time, min. |
| x | Fraction conversion of solid |
| β, ν | Physical parameters of the solid defined in Equation 3 |

Acknowledgment

This work was supported by grants from the Energy Research and Development Administration, Morgantown Energy Research Center. The authors wish to thank Nancy Tsai Wu for measuring some of the pore characteristics presented in this report and also A. G. Panson and G. E. Chidister for char analysis.

Literature Cited

1. Austin, L. G. and Walker, P. L., Jr., A.I.Ch.E. Journal, 9, 303 (1963).
2. Essenhigh, R. H. and Howard, J. B., Ind. Eng. Chem., 58 (1), 15 (1966).
3. Gray, D., Cogoli, J. G. and Essenhigh, R. H., Amer. Chem. Soc., Division of Fuel Chem. preprint, 18 (1), 135, Dallas (1973).
4. Gulbransen, E. A. and Andrew, K. F., Ind. Eng. Chem., 44, 1039 (1952).
5. Long, F. J. and Sykes, K. W., Proc. Roy. Soc. (London), 193A, 377 (1948).
6. Petersen, E. E., Walker, P. L., Jr., and Wright, C. C., Ind. Eng. Chem., 47, 1629 (1955).
7. Rossberg, M. and Wicke, E., Chem. Eng. Tech., 28, 181 (1956).
8. Turkdogan, E. T., Olsson, R. G. and Vinters, J. V., Carbon, 8, 545 (1970).
9. Turkdogan, E. T. and Vinters, J. V., Carbon, 7, 101 (1969).
10. Walker, P. L. Jr., Foresti, R. J., Jr., and Wright, C. C., Ind. Eng. Chem., 45, 1703 (1953).
11. Wen, C. Y., Bailie, R. C., Lin, C. Y. and O'Brien, W. S., Advances in Chemistry Series, 9, 131 (1974).
12. Wicke, E., Fifth Symp. on Combustion, p. 245, Reinhold, New York (1955).
13. Yoshida, K. and Kunii, D., J. Chem. Eng. (Japan), 2, 170 (1969).

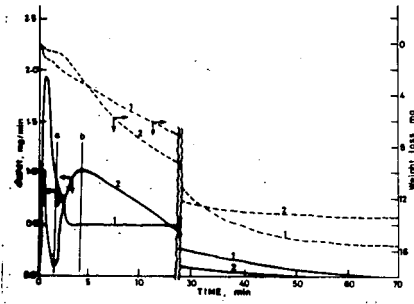


Fig. 1 Reproduction of Two Typical Chart Recordings of the Weight Loss and Rate of Weight Loss Curves
1--Hydrane Char #150, 2--Hydrane Char #49, Temperature: 1875°F.

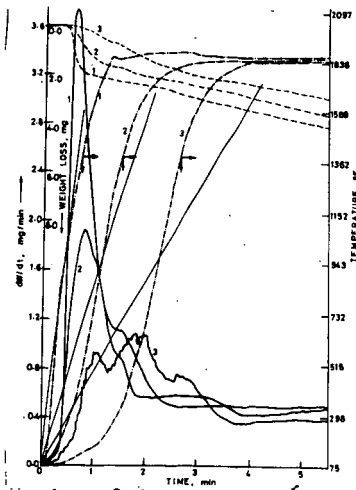


Fig. 3 Effect of Sample Heating Rate on the Pyrolysis of Hydrane Char #150, Sample size: 18.30 mg.

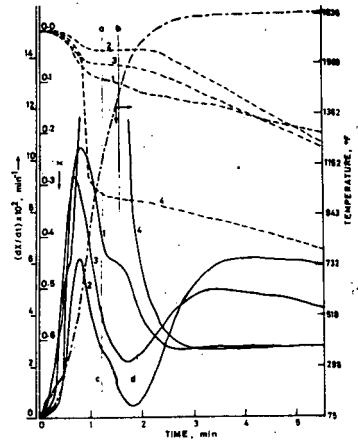


Fig. 2 Typical Rate and Conversion Curves for the Pyrolysis of Coal and Chars,

--- Conversion Versus Time Curve
— Rate Versus Time Curve
--- Temperature Versus Time Curve

1--Hydrane Char #150, 2--Hydrane Char #49, 3--Synthane Char #122, 4--Illinois Coal #6.

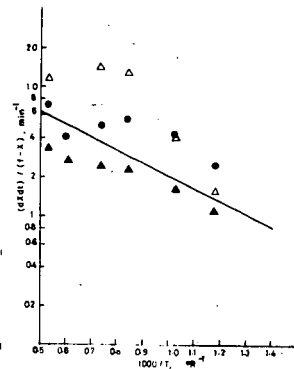


Fig. 4 Arrhenius Plot for the Pyrolysis Stage

▲ Hydrane Char #150, $f=0.110$
△ Hydrane Char #49, $f=0.0369$
● Synthane Char #122, $f=0.0675$

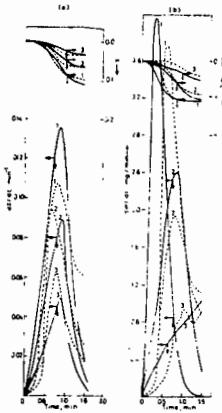


Fig. 5 Calculated (—) and Experimental (---) Rate and Conversion Curves, (a) For Different Char Samples: 1-Hydrane Char #150, 2-Synthane Char #122, 3-Hydrane Char #49; (b) For Different Heating Rates for Hydrane Char #150: The numbers 1, 2 and 3 correspond to the heating rate curves shown in Fig. 3.

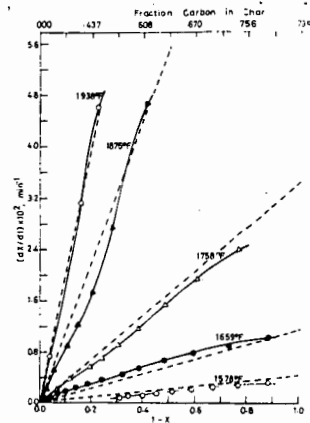


Fig. 6 Gasification of Hydrane Char #49, Rate Versus Conversion Based on Base-Carbon ---Calculated Rates.

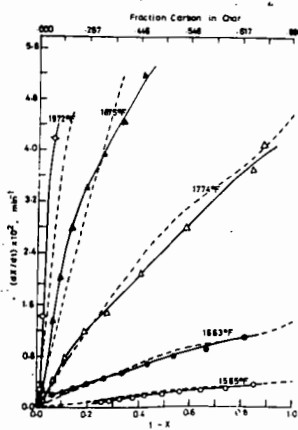


Fig. 7 Gasification of Synthane Char #122, Rate Versus Conversion Based on Base-Carbon ---Calculated Rates.

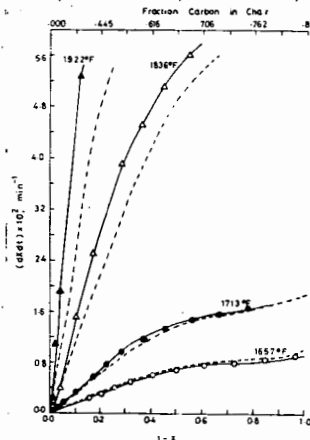


Fig. 8 Gasification of IGT Char #HT155, Rate Versus Conversion Based on Base-Carbon ---Calculated Rates.

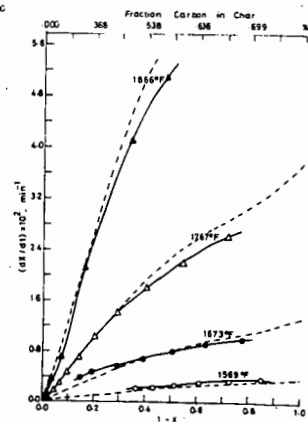


Fig. 9 Gasification of Illinois Coal #6, Rate Versus Conversion Based on Base-Carbon ---Calculated Rates.

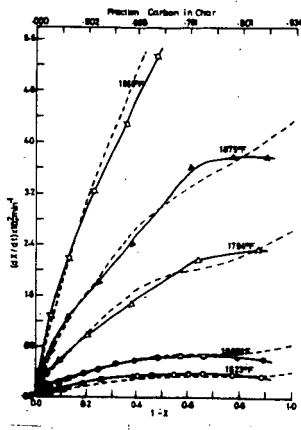


Fig. 10 Gasification of Hydrane Char #150, Rate Versus Conversion Based on Base-Carbon
----Calculated Rates.

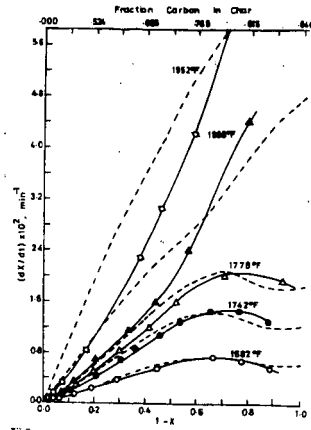


Fig. 11 Gasification of Pittsburgh HVab Coal, Rate Versus Conversion Based on Base-Carbon
----Calculated Rates.

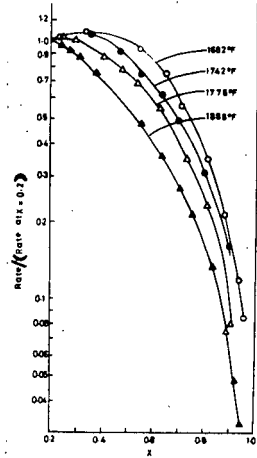


Fig. 12 Normalized Rates Versus Conversions for Pittsburgh HVab Coal.

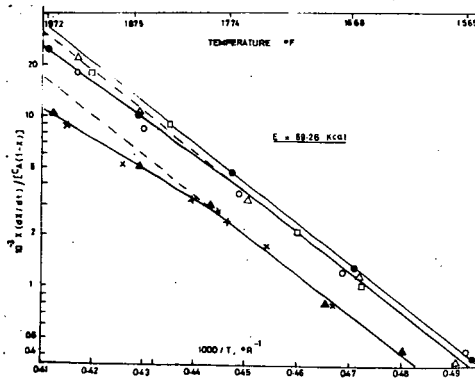


Fig. 13 Arrhenius Plots for Gasification of Coals and Chars

- Illinois Coal #6 △ Hydrane Char #49
- Synthane Char #122 □ IGT Char #HT155
- × Pittsburgh HVab Coal ▲ Hydrane Char #150

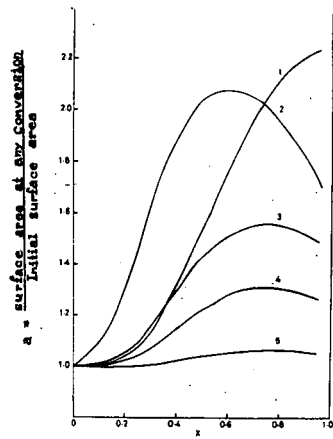


Fig. 14 Relative Available Surface Area Versus Conversion
1. Hydrane Char #150
2. Pittsburgh HVab Coal
3. IGT Char #HT155
4. Illinois Coal #6 & Synthane Char #122
5. Hydrane Char #49.